Neurobiology of Disease 58 (2013) 49–56

Contents lists available at SciVerse ScienceDirect

Neurobiology of Disease

journal homepage: www.elsevier.com/locate/ynbdi

Ataxin-3 protein modification as a treatment strategy for spinocerebellar ataxia type 3: Removal of the CAG containing exon

Melvin M. Evers [a], Hoang-Dai Tran [a], Ioannis Zalachoras [b], Barry A. Pepers [a], Onno C. Meijer [b], Johan T. den Dunnen [a,c,d], Gert-Jan B. van Ommen [a], Annemieke Aartsma-Rus [a], Willeke M.C. van Roon-Mom [a,*]

[a] Department of Human Genetics, Leiden University Medical Center, The Netherlands
[b] Department of Endocrinology, Leiden University Medical Center, The Netherlands
[c] Leiden Genome Technology Center, Leiden University Medical Center, The Netherlands
[d] Department of Clinical Genetics, Leiden University Medical Center, The Netherlands

ARTICLE INFO

Article history:
Received 1 March 2013
Revised 17 April 2013
Accepted 21 April 2013
Available online 6 May 2013

Keywords:
Spinocerebellar ataxia type 3
Polyglutamine disorder
Ataxin-3
Exon skipping
CAG repeat
Polyglutamine repeat

ABSTRACT

Spinocerebellar ataxia type 3 is caused by a polyglutamine expansion in the ataxin-3 protein, resulting in gain of toxic function of the mutant protein. The expanded glutamine stretch in the protein is the result of a CAG triplet repeat expansion in the penultimate exon of the *ATXN3* gene. Several gene silencing approaches to reduce mutant ataxin-3 toxicity in this disease aim to lower ataxin-3 protein levels, but since this protein is involved in deubiquitination and proteasomal protein degradation, its long-term silencing might not be desirable. Here, we propose a novel protein modification approach to reduce mutant ataxin-3 toxicity by removing the toxic polyglutamine repeat from the ataxin-3 protein through antisense oligonucleotide-mediated exon skipping while maintaining important wild type functions of the protein. *In vitro* studies showed that exon skipping did not negatively impact the ubiquitin binding capacity of ataxin-3. Our *in vivo* studies showed no toxic properties of the novel truncated ataxin-3 protein. These results suggest that exon skipping may be a novel therapeutic approach to reduce polyglutamine-induced toxicity in spinocerebellar ataxia type 3.

Introduction

Spinocerebellar ataxia type 3 (SCA3), also known as Machado–Joseph disease (MJD), is one of nine known polyglutamine (polyQ) disorders. PolyQ disorders are autosomal dominant neurodegenerative disorders caused by expansion of a CAG triplet in the coding region of a gene. This CAG repeat is translated into an extended glutamine stretch in the mutant protein, which causes a gain of toxic function inducing neuronal loss in various regions throughout the brain (Bauer and Nukina, 2009). A hallmark of all polyQ disorders is the formation of large insoluble protein aggregates containing the expanded disease protein. Whether these large aggregates are neurotoxic or neuroprotective is still under debate (Takahashi et al., 2010).

In SCA3, the CAG repeat is located in the penultimate exon of the *ATXN3* gene on chromosome 14q32.1. Healthy individuals have a CAG repeat ranging from 10 to 51, whereas SCA3 patients have an expansion of 55 repeats or more (Cummings and Zoghbi, 2000). Transgenic mice expressing either a mutant ataxin-3 cDNA fragment (Ikeda et al., 1996) or the mutated full-length genomic sequence (Cemal et al., 2002; Goti et al., 2004), showed a clear ataxic phenotype with a more severe phenotype in the animals carrying larger repeats (Bichelmeier et al., 2007), demonstrating a relationship between CAG repeat length and disease severity. The *ATXN3* gene codes for the ataxin-3 protein of 45 kDa, which acts as an isopeptidase and is thought to be involved in deubiquitination and proteasomal protein degradation (Burnett et al., 2003; Schmitt et al., 2007; Scheel et al., 2003). The ataxin-3 protein contains an N-terminal Josephin domain that displays ubiquitin protease activity and a C-terminal tail with 2 or 3 ubiquitin interacting motifs (UIMs), depending on the isoform (Goto et al., 1997). Although in the past decade there has been

Abbreviations: SCA3, spinocerebellar ataxia type 3; MJD, Machado–Joseph disease; PolyQ, polyglutamine; *ATXN3*, ataxin-3; UIMs, ubiquitin interacting motifs; RNAi, RNA interference; AON, antisense oligonucleotide; SNP, single nucleotide polymorphism; DMD, Duchenne muscular dystrophy; NES, nuclear export signal; ICV, intra-cerebral ventricular; NLS, nuclear localization signal; VCP, valosin containing protein.

* Corresponding author at: Department of Human Genetics, Leiden University Medical Center, Albinusdreef 2, 2333ZA Leiden, The Netherlands. Fax: +31 71 5268285.
E-mail addresses: M.M.Evers@lumc.nl (M.M. Evers), hoangdai_tran@yahoo.com (H.-D. Tran), I.Zalachoras@lumc.nl (I. Zalachoras), B.A.Pepers@lumc.nl (B.A. Pepers), O.C.Meijer@lumc.nl (O.C. Meijer), ddunnen@humgen.nl (J.T. den Dunnen), G.J.B.van_Ommen@lumc.nl (G.-J.B. van Ommen), A.M.Aartsma-Rus@lumc.nl (A. Aartsma-Rus), w.vanroon@lumc.nl (W.M.C. van Roon-Mom).

Available online on ScienceDirect (www.sciencedirect.com).

0969-9961 © 2013 The Authors. Published by Elsevier Inc. Open access under CC BY-NC-ND license.
http://dx.doi.org/10.1016/j.nbd.2013.04.019

extensive research into the SCA3 disease mechanisms (Matos et al., 2011), it is still not completely understood how the ataxin-3 polyQ expansion results in the observed pathology.

The most promising recent therapeutic strategy under development for polyQ disorders is reducing levels of mutant polyQ proteins using RNA interference (RNAi) and antisense oligonucleotides (AONs). As potential gene silencing treatment for SCA3, non-allele specific reduction of ataxin-3 has been tested in both mice (Schmitt et al., 2007) and rats (Alves et al., 2010). The treated rodents were viable and displayed no overt phenotype, suggesting that ataxin-3 is a non-essential protein. However, ataxin-3 might also have a protective role, since in flies ataxin-3 was found to alleviate neurodegeneration induced by mutant polyQ proteins (Warrick et al., 2005). Whether this is also true in humans is not known. The results in flies favor selective inhibition of mutant ataxin-3 protein levels over a total reduction of ataxin-3 protein levels. Successful allele-specific reduction of the mutant ataxin-3 transcript was shown using lentiviral small hairpin RNAs directed against a single nucleotide polymorphism (SNP) in the *ATXN3* gene *in vitro* (Miller et al., 2003) and *in vivo* (Alves et al., 2008; Nobrega et al., 2013). However, this approach is limited to SCA3 patients carrying a heterozygous SNP in the *ATXN3* gene. Semi-allele-specific reduction of mutant ataxin-3 has also been achieved by targeting the expanded CAG repeat using single stranded AONs *in vitro* (Evers et al., 2011; Hu et al., 2009; Hu et al., 2011).

We here introduce a novel way to reduce toxicity of the ataxin-3 protein through protein modification. Using AONs it is possible to mask exons in the pre-mRNA from the splicing machinery resulting in exclusion of the targeted exon (Spitali and Aartsma-Rus, 2012; Zalachoras et al., 2011). If the reading frame remains intact, subsequent translation yields an internally truncated protein. This has the major advantage that the polyQ-containing part of the protein is removed, while maintaining global ataxin-3 protein levels. AON-mediated exon skipping is a promising therapeutic tool that is already in phase II/III clinical trial for Duchenne muscular dystrophy (DMD) (van Putten and Aartsma-Rus, 2011; Cirak et al., 2011).

In this study we used 2′-O-methyl modified AONs with a phosphorothioate backbone to induce an in-frame exon skip in the ataxin-3 pre-mRNA. This resulted in a modified ataxin-3 protein lacking the polyQ repeat, while total ataxin-3 protein levels were unaltered and its functional domains remained intact. We showed that this modified protein retains its ubiquitin binding capacity. No cell death was seen after exon skipping, suggesting this modified protein did not induce *in vitro* toxicity. Injection of a single dose of AONs in the mouse cerebral ventricle resulted in exon skipping in the cerebellum, the brain area most affected in SCA3. These results suggest exon skipping could be a promising novel therapeutic approach to reduce polyglutamine-induced toxicity in SCA3.

Material and methods

Cell culture and transfection

Patient derived fibroblasts from SCA3 patients (GM06151, purchased from Coriell Cell Repositories, Camden, USA) and controls (FLB73, a kind gift from Dr. M.P.G. Vreeswijk, LUMC) were cultured at 37 °C and 5% CO_2 in Minimal Essential Medium (MEM) (Gibco Invitrogen, Carlsbad, USA) with 15% heat inactivated Fetal Bovine Serum (FBS) (Clontech, Palo Alto USA), 1% Glutamax (Gibco) and 100 U/ml penicillin/streptomycin (P/S) (Gibco). Mouse myoblasts C_2C_{12} (ATCC, Teddington, UK) were cultured in Dulbecco's Modified Eagle Medium (DMEM) (Gibco) with 10% FBS, 1% glucose, 2% Glutamax and 100 U/ml P/S.

AON transfection was performed in a 6-well plate with 3 μl of Lipofectamine 2000 (Life Technologies, Paisley, UK) per well. AON and Lipofectamine 2000 were diluted in MEM to a total volume of 500 μl and mixtures were prepared according to the manufacturer's instruction. Four different transfection conditions were used: 1) transfection with 1–200 nM AONs, 2) transfection with non-relevant h40AON2 directed against exon 40 of the *DMD* gene (Control AON) (Aartsma-Rus et al., 2002), 3) transfection with scrambled AON (Scrambled), and 4) transfection without AON (Mock) (for AON sequences, see Table 1). Mixtures were added to a total volume of 1 ml of MEM. Four hours after transfection, medium was replaced with fresh medium containing 5% FBS. All AONs consisted of 2′-O-methyl RNA and contained a full-length phosphorothioate modified backbone (Eurogentec, Liege, Belgium).

Plasmids and mutations

Full length as well as AON9.2 and AON10 induced skipped ataxin-3 fragments were PCR-amplified with ATXN3-specific primers (see Table 2) and cloned into pIVEX 1.4 WG vector that contained 6 His-tags (His_6-ataxin-3 full length and His_6-ataxin-3Δ59aa, respectively). Three microgram of vector DNA was used as template for cell free protein production using the RTS 100 kit together with the RTS ProteoMaster (Roche). His_6-tagged beta-glucuronidase (GUS) (5 Prime) was taken along as control vector.

Leucine to alanine mutations in the UIMs were performed using the QuikChange II Site-Directed Mutagenesis kit (Agilent Technologies, Waldbronn, Germany) following manufacturer's instructions, using forward and reverse primers containing the desired mutation (see Table 2).

RNA analysis

Twenty four hours after the first transfection, total RNA was isolated from cells using the Aurum Total RNA Mini Kit (BioRad, Hercules, USA), with an on-column DNase treatment for 30 min. Brain tissue was homogenized using ceramic MagNA Lyser beads (Roche, Mannheim, Germany) by grinding in a Bullet Blender (Next Advance, Averill Park, USA) according to manufacturer's instructions. RNA was eluted in a 40 μl elution buffer and cDNA was synthesized from 1 μg total RNA using the Transcriptor First Strand cDNA Synthesis Kit with Random Hexamer primers at 65 °C (Roche).

PCR was performed using 2 μl cDNA, 10× PCR buffer with 1.5 mM $MgCl_2$ (Roche), 0.25 mM dNTPs, 10 pmol of both forward and reverse primer (Eurogentec), 1 U FastStart Taq DNA Polymerase (Roche), and PCR grade water to a final volume of 20 μl. PCR was performed with primers for human and mouse ataxin-3 (see Table 2). The PCR program started with a 4 min initial denaturation at 95 °C, followed by 35 cycles of 30 s denaturation at 95 °C, 30 s annealing at 59 °C, and 45 s elongation at 72 °C, after which a final elongation step was performed at 72 °C for 7 min. Lab-on-a-Chip was performed on the Agilent 2100 Bioanalyzer (Agilent Technologies), using the Agilent DNA 1000 Kit.

The qPCR was performed on RNA extracted from tissue isolated from mouse brain, using 2 μl of 5 times diluted cDNA, 20 times EvaGreen-qPCR dye (Biotium, Hayward, USA), 10 times PCR buffer with 1 mM $MgCl_2$ (Roche), 0.25 mM dNTPs (Roche), 2.5 pmol forward primer, 2.5 pmol reverse primer, 0.35 U FastStart Taq DNA Polymerase (Roche), and PCR grade water to a total volume of 10 μl. Primer pairs located in various exons of ataxin-3 were selected for

Table 1
Antisense oligonucleotide sequences used for transfection and injection.

AON name	Sequence (5′–3′)
AON9.1	GAGAUAUGUUUCUGGAACUACC
AON9.2	GCUUCUCGUCUCUUCCGAAGC
AON10	GCUGUUGCUGCUUUUGCUGCUG
Control AON	UCCUUUCAUCUCUGGGCUC
mAON9.1	GCUUCUCGUCUCCUCCGCAGC
mAON10	GAACUUGUGGUCGGUCUUUCAC
Scrambled AON	CUGAACUGGUCUACAGCUC

Table 2
Primer sequences used for Sanger sequencing, mutagenesis, and (quantitative) RT-PCR.

Target	Species	Primer name	Application	Sequence (5′–3′)
ATXN3	Human	hATXN3Ex8Fw1	RT-PCR	CCATAAAACAGACCTGGAACG
ATXN3	Human	hATXN3Ex11Rev1	RT-PCR	ACAGCTGCCTGAAGCATGTC
ATXN3	Human	hATXN3_SDM_L229AFw	Mutagenesis	ACGAAGATGAGGAGGATGCGCAGAGGGCTCTGGC
ATXN3	Human	hATXN3_SDM_L229ARev	Mutagenesis	GCCAGAGCCCTCTGCGCATCCTCCTCATCTTCGT
ATXN3	Human	hATXN3_SDM_L249AFw	Mutagenesis	ACATGGAAGATGAGGAAGCAGATGCCCGCAGGGCTAT
ATXN3	Human	hATXN3_SDM_L249ARev	Mutagenesis	ATAGCCCTGCGGGCATCTGCTTCCTCATCTTCCATGT
Atxn3	Mouse	mAtxn3Ex7Fw1	RT-PCR	AAGAGCAGAGTGCCCTCAAA
Atxn3	Mouse	mAtxn3Ex11Rev1	RT-PCR	TTTCTAAAGACATGGTCACAGC
Atxn3	Mouse	mAtxn3Ex4Fw1	qRT-PCR	TGCTTTGAAAGTTTGGGGTTT
Atxn3	Mouse	mAtxn3Ex4Rev1	qRT-PCR	CTGAGCCTCTGGTACTCTGGA
Atxn3	Mouse	mAtxn3Ex9Fw1	qRT-PCR	GTCCACAGACATCAAGTCCAGA
Atxn3	Mouse	mAtxn3Ex9Rev1	qRT-PCR	GTCTCCTCCGCAGCTCTTC
Atxn3	Mouse	mAtxn3Ex10Fw1	qRT-PCR	AGCAGCAGCAGGAGGTAGAC
Atxn3	Mouse	mAtxn3Ex10Rev1	qRT-PCR	CGTCCTCCTGAACTTGTGGT
Atxn3	Mouse	mAtxn3Ex11Fw1	qRT-PCR	ACCGACCACAAGTTCAGGAG
Atxn3	Mouse	mAtxn3Ex11Rev2	qRT-PCR	CCGAAGCATGTCCTCTTCAC
Rpl22	Mouse	mRpl22Ex3Fw1	qRT-PCR	AGGAGTCGTGACCATCGAAC
Rpl22	Mouse	mRpl22Ex3Rev1	qRT-PCR	TTTGGAGAAAGGCACCTCTG
Ywhaz	Mouse	mYwhazEx4Fw1	qRT-PCR	TCAGCAAAAAGGAGATGCAG
Ywhaz	Mouse	mYwhazEx4Rev1	qRT-PCR	TTTCTCTGGGGAGTTCAGGA

Abbreviations: ATXN3, ataxin-3; Rpl22, ribosomal protein L22; Ywhaz, tyrosine 3-monooxygenase/tryptophan 5-monooxygenase activation protein, zeta polypeptide.

qRT-PCR using Primer3 software (Rozen and Skaletsky, 2000) and tyrosine 3-monooxygenase/tryptophan 5-monooxygenase activation protein, zeta polypeptide (Ywhaz) and ribosomal protein L22 (Rpl22) were used as reference genes (for primer list, see Table 2). The qRT-PCR was performed using the LightCycler 480 (Roche). Initial denaturation was 10 min at 95 °C, followed by 45 cycles of 10 s denaturation at 95 °C, 30 s annealing at 60 °C and 20 s elongation at 72 °C. The final elongation was performed 5 min at 72 °C.

Primer efficiencies were determined using LinRegPCR v2012.0 with the raw data amplification curves as input. The raw data were baseline corrected and absolute transcript level expressions (N0) were calculated as described previously (Ruijter et al., 2009). All samples were run in triplicate on a plate. On all plates both reference genes were included to correct for inter-plate variance.

Sanger sequencing

Full length and skipped products were amplified using primers flanking ataxin-3 exon 9 and 10 (see Table 2). PCR products were loaded on agarose gel and bands were extracted using the QIAquick Gel Extraction Kit (QIAgen, Valencia, USA). The purified products were re-amplified, purified, and analyzed by Sanger sequencing, using the Applied Biosystems 96-capillary 3730XL system (Life Technologies Corporation, Carlsbad, USA) with the Applied Biosystems BigDyeTerminator v3.1 kit.

Protein isolation, ubiquitin binding assay and Western blotting

Cells were detached from the culture surface with a 0.5% Trypsin/EDTA solution. After washing twice with HBSS, cells were resuspended in 200 μl ice cold lysis buffer, containing 15 mM Hepes, pH 7.9, 200 mM KCl, 10 mM $MgCl_2$, 1% NP40, 10% glycerol, 20 μg/ml BSA, and 1 tablet complete mini protease inhibitor EDTA free (Roche) per 10 ml buffer. Next, samples were sonicated 3 times for 5 s using ultrasound with an amplitude of 60 at 4 °C. After 1 h incubation in a head-over-head rotor at 4 °C, the extract was centrifuged for 15 min at 10,000 *g* and 4 °C and the supernatant was isolated. Protein concentrations were determined by the bicinchoninic acid kit (Thermo Fisher Scientific, Waltham, USA) using Bovine Serum Albumin (BSA) as a standard. Samples were snap frozen and stored at −80 °C.

His_6-ataxin-full length and His_6-ataxin-3Δ59aa proteins were bound to TALON metal affinity beads (Clontech) for 30 min. The ataxin-3-bound beads were incubated at 4 °C with 5 μg poly-ubiquitin chains (Enzo Life Sciences, Farmingdale, USA). Binding reactions contained 15 mM Hepes, pH 7.9, 200 mM KCl, 10 mM $MgCl_2$, 1% NP40, 10% glycerol, and 20 μg/ml BSA. Beads were washed extensively and bound proteins were removed from the beads by 2 h incubation at 23 °C with 2 μg Factor Xa Protease (New England Biolabs, Ipswich, United Kingdom) per reaction.

Protein extracts were separated by SDS-PAGE, with 10% acryl/bisacrylamide 1:37.5 separating gels, or Any kD precast TGX gels (BioRad). For each gel the PageRuler prestained protein ladder (Thermo Fisher Scientific) was used as marker. Electrophoresis was performed until the lowest marker reached the bottom of the gel. Gels were blotted onto nitrocellulose membranes using the Transblot Turbo (BioRad) for 30 min at 2.5 A. Membranes were blocked with Tris Buffered Saline (TBS) containing 5% non-fat milk powder (Profitar Plus, Nutricia, Zoetermeer, the Netherlands).

The mouse SCA3-1H9 antibody was used for detecting ataxin-3 (Millipore, Billerica, USA), dilution 1:1000, or rabbit His-tag 2365 (Cell Signaling Technology, Danvers, USA). To detect expanded polyQ stretches we used mouse 1C2 (Eurogentec), dilution 1:500. To detect ubiquitin chains, we used rabbit ubiquitin–protein conjugates (Enzo Life Sciences), diluted 1:2000. Secondary antibodies were goat α-mouse-IRDye800, goat α-rabbit-IRDye800 (LI-COR Biosciences, Lincoln, USA), and goat α-mouse-horseradish peroxidase (HRP) (Santa Cruz Biotechnology, USA), diluted 1:5000 in block buffer. Horseradish peroxidase was activated by ECL+ reagent (GE Healthcare, Buckinghamshire, United Kingdom) to visualize positive staining on film or an Odyssey scanner (LI-COR) was used to visualize infrared bands. Intensities of protein bands were quantified using Odyssey software. The skipping efficiencies were calculated as described in the calculations and statistical analysis paragraph.

AON injection into mice

Mouse ataxin-3 specific AONs (mAON9.1 and mAON10) and scrambled control AONs (Table 1) were injected in anesthetized 12–14 week old C57bl/6j male mice (Janvier SAS, France). Animals were singly housed in individually ventilated cages (IVC) at a 12 hour light cycle with lights on at 7 am. Food and water were available *ad libitum*. All animal experiments were carried out in accordance with the European Communities Council Directive 86/609/EEC and the Dutch law on animal experiments and were approved by the Leiden University animal ethical committee (protocol number: 12186). A total of 40 μg AON mix diluted in 5 μl sterile saline was

injected into the left lateral ventricle at 0.22 mm anterior–posterior, 1.5 mm medio-lateral, and −2.5 mm dorso-ventral relative to bregma, using borosilicate glass micro-capillary tips connected to a Hamilton syringe (5 μl, 30 gauge). The Hamilton syringe was connected to an injection pump (Harvard apparatus, Holliston, MA, USA), which controlled the injection rate set at 0.5 μl/min. After 7 days the mice were sacrificed and the brains were isolated and frozen for qRT-PCR analysis.

Calculations and statistical analysis

RNA and protein skipping percentages were calculated using the following formula: Skipping% = (molarity skipped product / (total molarity full length product + skipped product)) * 100%. The skipping percentages were analyzed using a paired two-sided Student *t*-test. Differences were considered significant when $P < 0.05$.

Results

AON mediated skipping of ataxin-3 exon 9 and 10 in vitro

The CAG repeat in the *ATXN3* gene is located in exon 10, which is 119 nucleotides in length. Thus skipping will disrupt the reading frame. To preserve the reading frame exon 9 (97 nucleotides) and 10 need to be skipped simultaneously. Various AONs were designed targeting exon internal sequences of ataxin-3 exon 9 and 10 and transfected in human fibroblasts (Table 1). PCR analysis revealed a 97 nucleotide skip after transfection with 100 nM of AON9.1 (efficiency = 59.2% ± 1.0%) (Figs. 1A and B). Sanger sequencing confirmed that this was a skip of exon 9. Transfection with 100 nM AON9.2 resulted in a skip of 55 nucleotides (efficiency = 62.3% ± 3.7%) instead of the anticipated 97 nucleotides (Figs. 1A and C). Sanger sequencing revealed that this fragment was a partial skip product that still contained the 5′ part of exon 9. *In silico* analysis showed the existence of a cryptic 5′ splice site AG|GTCCA in exon 9 that could explain the occurrence of this shorter fragment (Zhang, 1998). Successful skipping of exon 10 was achieved with 50 nM AON10 (efficiency = 96.3% ± 0.3%) (Figs. 1A and D), as confirmed by Sanger sequencing.

Co-transfection of AON9.1 and AON10 and AON9.2 and AON10 resulted in a skip of respectively 216 and 174 nucleotides (Fig. 2). The efficiency of the AON9.1 and AON10 induced double skip was 77.0% (±0.9%) in control fibroblasts (Figs. 2D and E). The efficiency of AON9.2 and AON10 co-transfection was 97.8% (±0.8%) in control fibroblasts (Figs. 2D and E). The unexpected in-frame partial skip of exon 9 with AON9.2 resulted in an alternative approach to remove the CAG repeat containing exon from the ataxin-3 transcript (Fig. 2).

Modified ataxin-3 protein maintains it ubiquitin binding capacity

To investigate if AON transfection resulted in a modified ataxin-3 protein, control and SCA3 fibroblasts were transfected with AONs targeting exon 9 and 10 and protein was isolated three days after transfection. We did not see a negative effect on cell viability after AON treatment in either control or SCA3 fibroblasts (Fig. S1). Western blot analysis using an ataxin-3-specific antibody revealed a modified band of approximately 35 kDa after the complete skip of exon 9 and 10 (ataxin-3 Δ72aa) (Fig. 3A); 11.4% (±5.1%) and 6.2% (±1.9%) of total ataxin-3 protein levels consisted of this modified ataxin-3 Δ72aa protein, in respectively control and SCA3 fibroblasts (Figs. 3B and C).

The partial exon skip resulted in a novel 37 kDa protein (ataxin-3 Δ59aa) (Fig. 3A). 27.1% (±9.0%) and 15.9% (±3.2%) of total ataxin-3 protein levels consisted of this 59 amino acids shorter ataxin-3 protein, in respectively control and SCA3 cells (Figs. 3B and C). The ataxin-3 Δ72aa protein was also formed, suggesting that AON9.2 and AON10 transfection also resulted in some ataxin-3 Δ72aa protein. The consistent lower percentage of exon skipping in SCA3 cells were caused by the lower AON transfection efficiencies in the diseased cells as compared to control cells.

A significant reduction in expanded polyQ containing ataxin-3 was shown using the 1C2 antibody, that recognizes long glutamine stretches (Trottier et al., 1995) (Fig. 3A) in the samples with the full and partial exon skip approaches. This indicates a reduction of expanded polyQ-containing ataxin-3 in SCA3 patient derived fibroblasts after AON transfection.

The polyQ repeat in the ataxin-3 protein is located between the second and third UIM (Fig. 4A). Both full and partial exon skip approaches resulted in the removal of the polyQ repeat, preserving the Josephin domain, nuclear export signal (NES), and UIMs. To investigate whether the ubiquitin binding capacities of the UIMs in ataxin-3 are still intact after protein modification, poly-ubiquitin chains were incubated with purified cell free produced full-length ataxin-3 and ataxin-3 Δ59aa protein. As negative controls, we produced 3 different ataxin-3 protein products containing 1 amino acid substitutions from leucine (L) to alanine (A) in UIM 1 (L229A), UIM 2 (L249A), or both (L229A/L249A) (Fig. 4B). Single amino acid changes in UIM 1 (L229A) already showed reduced binding of ataxin-3 to poly-ubiquitin chains, whereas double UIM mutated ataxin-3 (L229A/L249A) resulted in a nearly complete elimination poly-ubiquitin binding (Fig. 4C). This is consistent with previously described data (Burnett et al., 2003). The negative HIS control protein did not bind ubiquitylated proteins as expected. Ataxin-3 Δ59aa bound poly-ubiquitin chains comparable to full-length ataxin-3, indicating that its ubiquitin binding capacity after protein modification is still intact (Fig. 4C).

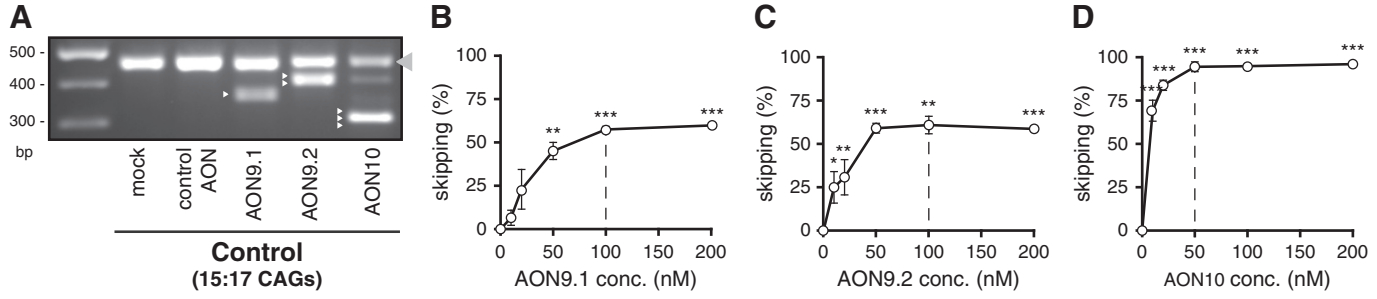

Fig. 1. Single exon skipping of ataxin-3 pre-mRNA *in vitro*. Control fibroblasts were transfected with ataxin-3 AONs, control AON, and non-transfected (mock) and RNA was isolated after 24 h. (A) Agarose gel analysis of the ataxin-3 transcript with primers flanking exon 9 and 10 (full-length, gray arrowhead). Transfection with 50 nM AON against exon 9 resulted in a product lacking the entire exon 9 (AON9.1, white arrowhead) or lacking the 3′ part of exon 9 (AON9.2, two white arrowheads). Transfection with 50 nM AON10 resulted in a product lacking exon 10 (three white arrowheads). Fibroblasts were transfected with concentrations ranging from 10 to 200 nM per ataxin-3 AON and Lab-on-a-Chip analysis was performed to calculate exon skip levels for (B) AON9.1, (C) AON9.2, and (D) AON10. Mean ± SD, data were evaluated using paired student *t*-test, $^{*}P < 0.05$, $^{**}P < 0.01$, $^{***}P < 0.001$, relative to mock transfection, n = 4.

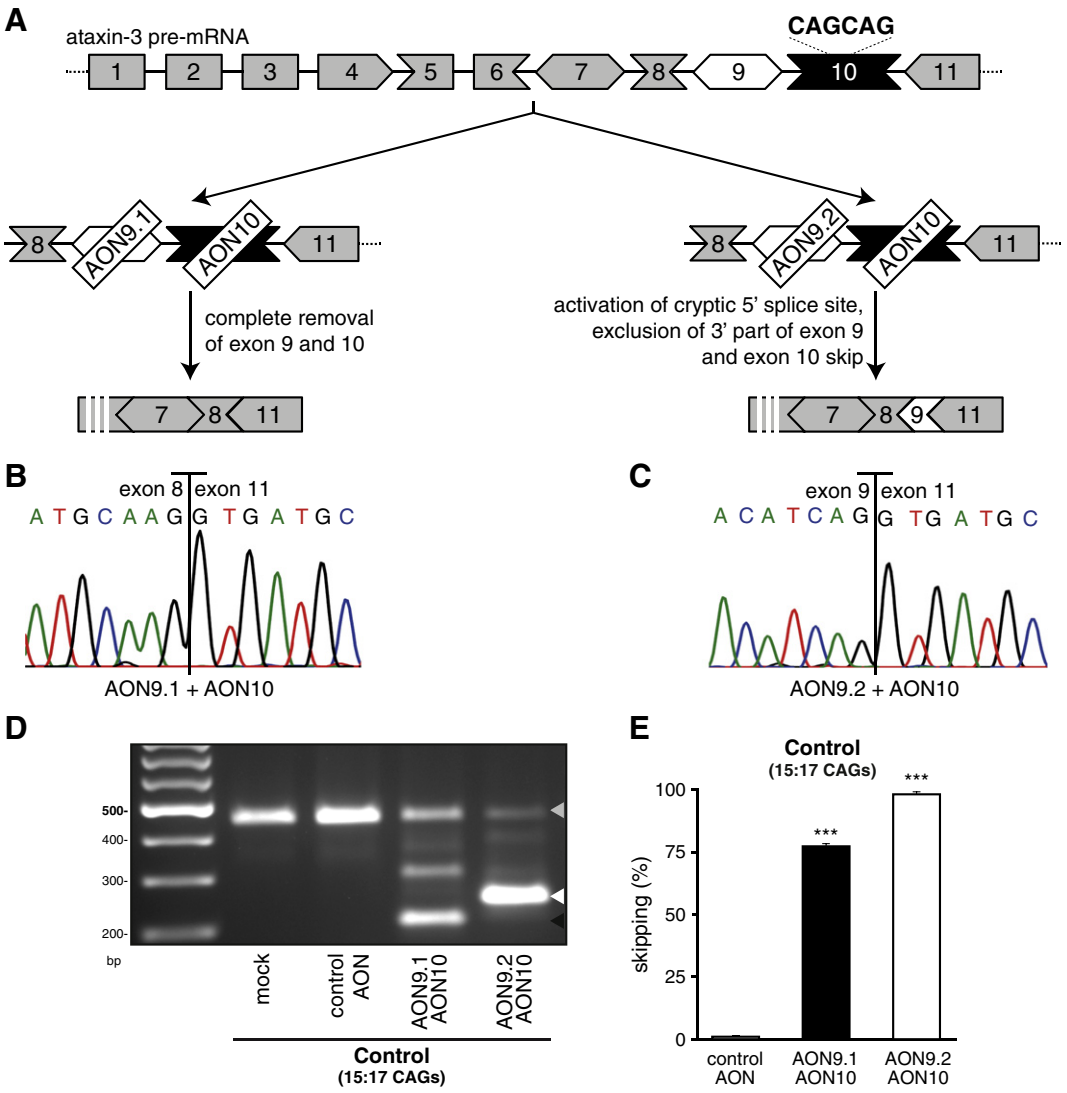

Fig. 2. Double exon skipping of ataxin-3 pre-mRNA *in vitro*. (A) Schematic representation of two approaches to induce in-frame skipping of the CAG repeat-containing exon. (B) Skip of exon 9 and 10 (AON9.1 + AON10) confirmed by Sanger sequencing. (C) Partial skip of exon 9 and complete skip of exon 10 (AON9.2 + AON10) confirmed by Sanger sequencing. (D) Agarose gel analysis of the ataxin-3 transcript with primers flanking exon 9 and 10. Transfection of control fibroblasts resulted in a product lacking both exon 9 and 10 (AON9.1 + AON10, black arrowhead) or lacking the 3′ part of exon 9 and exon 10 (AON9.2 + AON10, white arrowhead). (E) Lab-on-a-Chip analysis was performed to calculate exon skip levels in control cells. Mean + SD, data were evaluated using paired student *t*-test, $^{**}P < 0.01$, $^{***}P < 0.001$, relative to mock, n = 4.

AON mediated skipping of ataxin-3 exon 9 and 10 in mouse

To examine ataxin-3 exon skipping in the mouse brain and to determine if the modified protein is not harmful, we designed AONs specific to the mouse sequence. Since mice do not exhibit the cryptic splice site that is responsible for the partial exon 9 skip in the human transcript, we only investigated the full skip of exon 9 and 10. Transfection of 200 nM of each murine AON9 (mAON9) and AON10 (mAON10) in mouse C_2C_{12} cells showed a skip of both exons with an efficiency of 31.7% (±2.4%) (Fig. 5A). Sanger sequencing confirmed this in-frame double exon skip (Fig. 5B). Transfection with mAON9 and mAON10 resulted in formation of a modified protein of 34 kDa (Fig. 5C).

Next, a single intra-cerebral ventricular (ICV) injection was administered of 40 μg ataxin-3 AON mix (20 μg per AON) or 40 μg scrambled AON. After 7 days the mice were sacrificed and skipping efficiency in the cerebellum was assessed by qRT-PCR (Fig. 6). Exon 9 was found significantly reduced by 44.5% (±7.6%) and exon 10 was reduced by 35.9% (±14.1%) after a single ICV injection of AONs as compared to scrambled AON. Exon 4, upstream, and exon 11, downstream of the area targeted for skipping were not reduced, demonstrating a specific skip of ataxin-3 exon 9 and 10 *in vivo*.

Discussion

In the current study we show a novel approach to reduce toxicity of the mutant ataxin-3 protein through skipping of the CAG repeat containing exon in the ataxin-3 transcript. The resulting modified ataxin-3 protein lacks the polyQ repeat that is toxic when expanded, but maintains its ubiquitin binding properties. ICV administration of these AONs in mice resulted in skipping of the CAG repeat-containing exon in the cerebellum of control mice, proving distribution and efficiency of ataxin-3 exon skipping after ICV injection *in vivo*.

There was no negative effect on cell viability after AON treatment in both control and SCA3 fibroblasts and also no overt toxicity *in vivo*. There are several known important functional domains in ataxin-3 that have been implicated to be involved in the SCA3 pathogenesis. Skipping of exon 9 and 10 described here resulted in the removal of sequences encoding the calcium-dependent calpain cleavage and

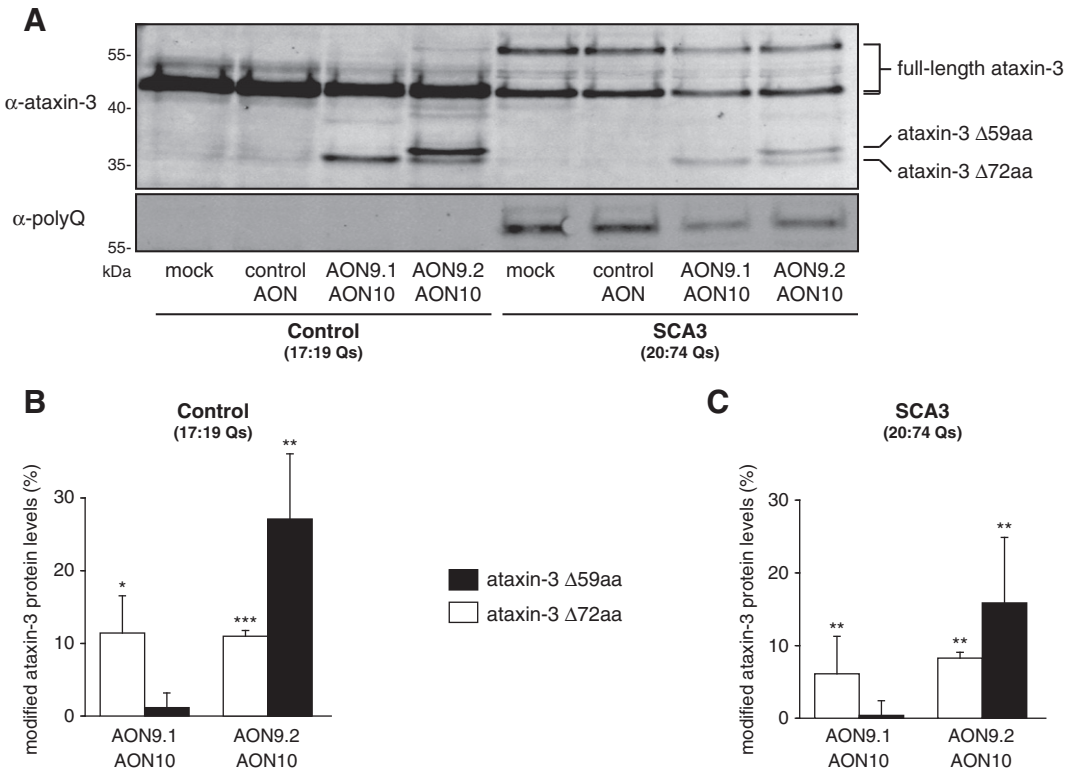

Fig. 3. Modified ataxin-3 protein after exon 9 and 10 skipping. Human control and SCA3 fibroblasts were transfected with 50 nM of each AON. (A) Transfection with AON9.1 and AON10, or AON9.2 and AON10 resulted in modified ataxin-3 proteins of 35 kDa (ataxin-3 Δ72aa) and 37 kDa (ataxin-3 Δ59aa), respectively. The modified protein products were shown using an ataxin-3 specific antibody. The reduction in polyQ-containing mutant ataxin-3 was shown with the polyQ antibody 1C2. Densitometric analysis was used after transfection with AONs. Ataxin-3 Δ72aa (white bars) and ataxin-3 Δ59aa (black bars) in (B) control and (C) SCA3 cells. Mean + SD, data were evaluated using paired student *t*-test, $^{*}P < 0.05$, $^{**}P < 0.01$, $^{***}P < 0.001$, relative to mock, n = 5.

nuclear localization signal (NLS), both located in exon 9. Following to the weak NLS located in the C-terminus (Macedo-Ribeiro et al., 2009), the ataxin-3 protein has two strong NES located at the N-terminal part (Macedo-Ribeiro et al., 2009). In SCA3 it is thought that proteolytic cleavage of mutant ataxin-3 results in C-terminal fragments lacking the NES but containing the polyglutamine stretch, resulting in localization of the toxic C-terminal fragments into the nucleus and formation of nuclear inclusion bodies (Bichelmeier et al., 2007; Colomer Gould et al., 2007). Recent studies in a mutant N-terminal ataxin-3 mouse model showed that N-terminal fragments, lacking the NLS, reside in the cytosol and form cytoplasmic inclusion bodies with subsequent neuronal degeneration (Hubener et al., 2011). Both above described mutant C- and N-terminal ataxin-3 fragments could be the result of calpain cleavage at amino acid 260 (Haacke et al., 2007). Skipping of exon 9 and 10 will also result in the removal of an arginine/lysine-rich motif around amino acid 285 that was found to be a potential valosin containing protein (VCP) binding domain (Boeddrich et al., 2006; Doss-Pepe et al., 2003). The ataxin-3-VCP complex is thought to be involved in assisting targeted proteins to the proteasome (Wang et al., 2006). In flies, co-expression of mutant ataxin-3 and VCP, resulted in alleviation of ataxin-3 aggregation and neurotoxicity in photoreceptor neurons (Boeddrich et al., 2006). Whether the removal of the VCP binding domain by exon skipping causes impaired degradation of target substrates needs to be assessed in future studies.

As potential gene silencing treatment for SCA3, both non-allele and allele specific reduction of (mutant) ataxin-3 have been tested. The main advantage of the AON-based protein modification approach compared to existing gene silencing approaches is the preservation of overall ataxin-3 transcript and protein levels. Only the polyQ stretch and a small portion of the surrounding amino acids of the protein are removed and the N-terminal Josephine domain and C-terminal ubiquitin binding motifs are preserved. We validated this by showing that the modified ataxin-3 protein retains its normal ubiquitin binding function. Furthermore, the exon skipping approach described here has the advantage that one set of AONs can be applied to all SCA3 patients. This in contrast with a previously described SNP-specific approach (Miller et al., 2003; Alves et al., 2008) that is only applicable for 70% of the patients who have the targeted SNP in their *ATXN3* gene (Gaspar et al., 2001).

That AONs are a promising therapeutic tool was recently shown in phase I and phase I/II clinical trials in DMD (Goemans et al., 2011; Cirak et al., 2011). As treatment for neurodegenerative disorders, AONs with a phosphorothioate backbone are very promising and are currently tested in phase I and phase I/II clinical trials for amyotrophic lateral sclerosis (ClinicalTrials.gov, 2009) and, more recently, a phase I trial has been initiated for spinal muscular atrophy (Rigo et al., 2012). After injection into the cerebrospinal fluid in non-human primates, AONs diffuse to the brain areas that are affected most in SCA3 patients, which are the cerebellum, basal ganglia, and pons (Kordasiewicz et al., 2012). In transgenic HD mice, the most pronounced mutant huntingtin protein reduction was seen after AON infusion for a limited period of time. Furthermore, several months after the last AON infusions there were sustained phenotypic improvements (Kordasiewicz et al., 2012).

The above results are very promising but future experiments will have to determine the best route of administration to the brain, optimal dosage, and treatment regime. Future experiments are required to evaluate whether polyQ skipping improves the SCA3 induced phenotype using transgenic SCA3 mice. Furthermore, it will also be

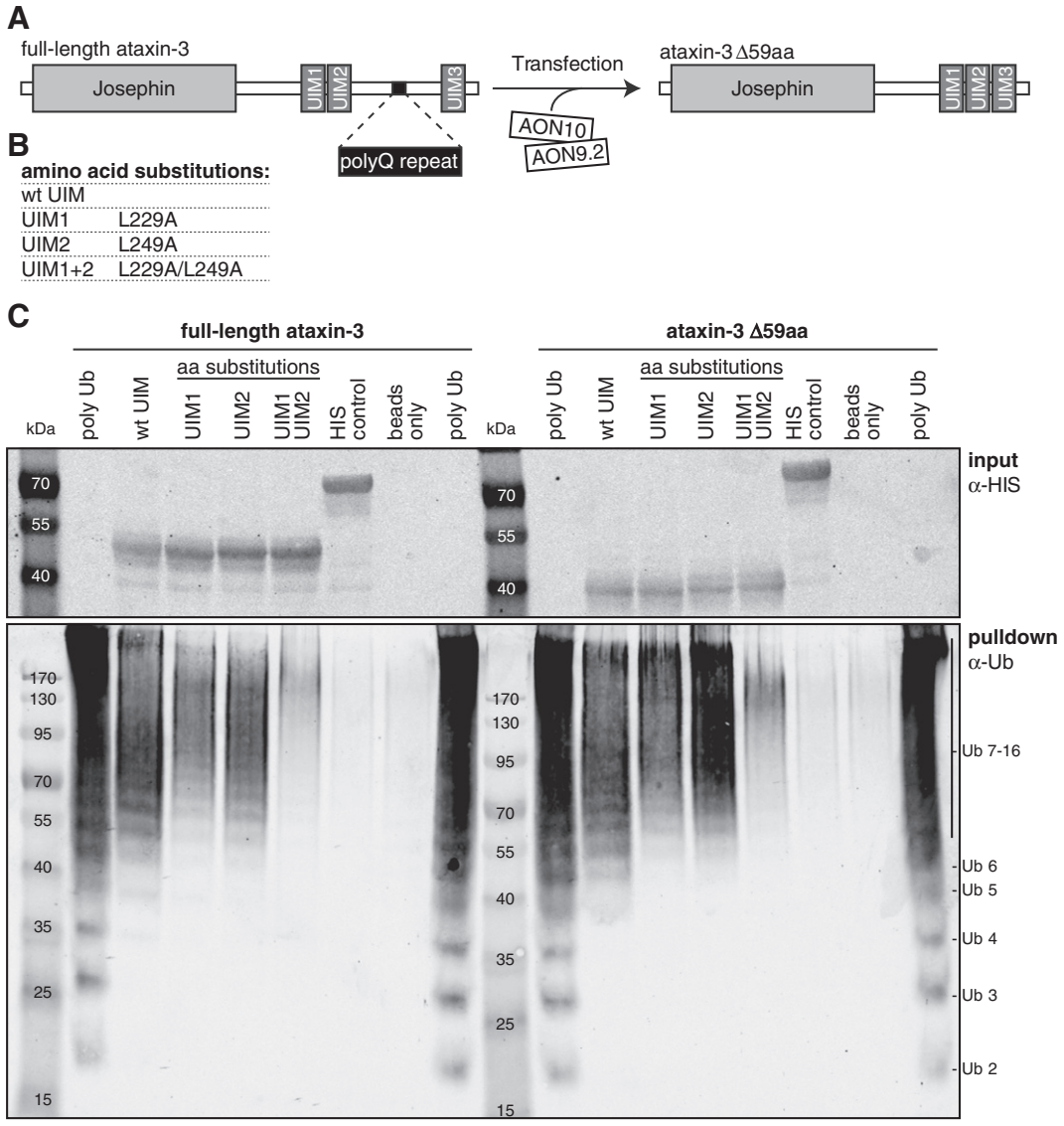

Fig. 4. Full-length and modified ataxin-3 protein displays identical ubiquitin binding. (A) Schematic representation of the known functional domains of the ataxin-3 protein involved in deubiquitination. The ataxin-3 protein consists of an N-terminal (Josephin) domain with ubiquitin protease activity and a C-terminal tail with the polyQ repeat and 3 ubiquitin interacting motifs (UIMs). After exon skipping (ataxin-3 Δ59aa), the polyQ repeat is removed, leaving the Josephin domain and UIMs intact. (B) Overview of a leucine (L) to alanine (A) substitution in UIM 1 (L229A), UIM 2 (L249A) or both (L229A/L249A) in full-length ataxin-3 and ataxin-3 Δ59aa. (C) Ubiquitin binding assay. His-tagged full-length ataxin-3 and ataxin-3 Δ59aa-bound ubiquitylated proteins were analyzed by Western blot. HIS control and beads only were taken along as negative control. The modified ataxin-3 Δ59aa lacking the polyQ repeat showed identical ubiquitylated protein binding as unmodified ataxin-3. (n = 3).

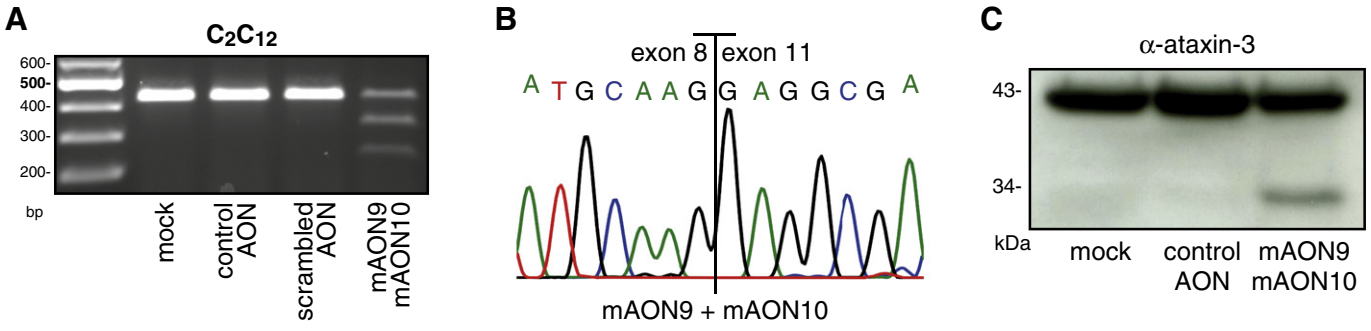

Fig. 5. Double exon skipping of murine ataxin-3 pre-mRNA *in vitro*. Mouse C_2C_{12} cells were transfected with murine ataxin-3 AONs, control AON, scrambled AON, and not transfected (Mock). (A) Agarose gel analysis of the ataxin-3 transcript with primers flanking exon 9 and 10. Skipping of ataxin-3 exon 9 and 10 was seen after transfection with mAON9.1 and mAON10. (B) Sanger sequencing confirmed the precise skipping of exon 9 and 10. (C) Transfection with mouse AON9.1 and AON10 resulted in the appearance of a modified ataxin-3 protein of 34 kDa.

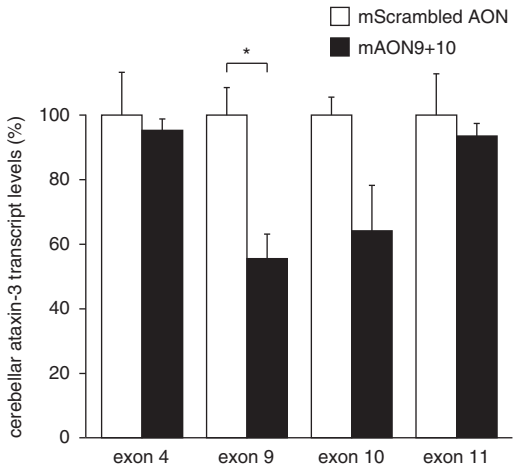

Fig. 6. Reduction of mouse ataxin-3 exon 9 *in vivo*. Seven days after a single injection consisting of mAON9 and mAON10 (20 μg each) into the mouse cerebral ventricle. qRT-PCR analysis of cerebellar tissue showed reduced exon 9 and 10 transcript levels, whereas exon 4 and 11 levels were not affected. Mean + SD, data were evaluated using paired student *t*-test, $^{*}P < 0.05$, n = 3.

necessary to assess whether the modified ataxin-3 protein is not toxic *in vitro* and *in vivo* and whether exon skipping results in altered localization, function, or aggregation.

In conclusion, we show that it is possible to remove the toxic polyQ repeat from a polyQ disease-causing protein and that this modified ataxin-3 protein exhibits regular ubiquitin binding. We also show the *in vivo* potential of this approach as CAG repeat-containing exon skip in the cerebellum was seen after a single ICV injection.

Supplementary data to this article can be found online at http://dx.doi.org/10.1016/j.nbd.2013.04.019.

Acknowledgments

The authors would like to thank Lodewijk Toonen and Nisha Verwey for technical assistance.

This work was supported by AtaxiaUK (United Kingdom), patiëntenvereniging Autosomaal Dominante Cerebellaire Ataxia (ADCA) (the Netherlands), the Center for Biochemical Genetics (the Netherlands), and Center for Medical Systems Biology (OCM/IZ).

References

Aartsma-Rus, A., Bremmer-Bout, M., Janson, A.A.M., den Dunnen, J.T., van Ommen, G.J.B., van Deutekom, J.C.T., 2002. Targeted exon skipping as a potential gene correction therapy for Duchenne muscular dystrophy. Neuromuscul. Disord. 12, S71–S77.

Alves, S., Nascimento-Ferreira, I., Auregan, G., Hassig, R., Dufour, N., Brouillet, E., et al., 2008. Allele-specific RNA silencing of mutant ataxin-3 mediates neuroprotection in a rat model of Machado–Joseph disease. PLoS One 3, e3341.

Alves, S., Nascimento-Ferreira, I., Dufour, N., Hassig, R., Auregan, G., Nobrega, C., et al., 2010. Silencing ataxin-3 mitigates degeneration in a rat model of Machado–Joseph disease: no role for wild-type ataxin-3? Hum. Mol. Genet. 19, 2380–2394.

Bauer, P.O., Nukina, N., 2009. The pathogenic mechanisms of polyglutamine diseases and current therapeutic strategies. J. Neurochem. 110, 1737–1765.

Bichelmeier, U., Schmidt, T., Hubener, J., Boy, J., Ruttiger, L., Habig, K., et al., 2007. Nuclear localization of ataxin-3 is required for the manifestation of symptoms in SCA3: *in vivo* evidence. J. Neurosci. 27, 7418–7428.

Boeddrich, A., Gaumer, S., Haacke, A., Tzvetkov, N., Albrecht, M., Evert, B.O., et al., 2006. An arginine/lysine-rich motif is crucial for VCP/p97-mediated modulation of ataxin-3 fibrillogenesis. EMBO J. 25, 1547–1558.

Burnett, B., Li, F., Pittman, R.N., 2003. The polyglutamine neurodegenerative protein ataxin-3 binds polyubiquitylated proteins and has ubiquitin protease activity. Hum. Mol. Genet. 12, 3195–3205.

Cemal, C.K., Carroll, C.J., Lawrence, L., Lowrie, M.B., Ruddle, P., Al-Mahdawi, S., et al., 2002. YAC transgenic mice carrying pathological alleles of the MJD1 locus exhibit a mild and slowly progressive cerebellar deficit. Hum. Mol. Genet. 11, 1075–1094.

Cirak, S., Arechavala-Gomeza, V., Guglieri, M., Feng, L., Torelli, S., Anthony, K., et al., 2011. Exon skipping and dystrophin restoration in patients with Duchenne muscular dystrophy after systemic phosphorodiamidate morpholino oligomer treatment: an open-label, phase 2, dose-escalation study. Lancet 378, 595–605.

ClinicalTrials.gov, 30-12-2009. Safety, Tolerability, and Activity Study of ISIS SOD1Rx to Treat Familial Amyotrophic Lateral Sclerosis (ALS) Caused by SOD1 Gene Mutations (SOD-1) (NCT01041222).

Colomer Gould, V.F., Goti, D., Pearce, D., Gonzalez, G.A., Gao, H., Bermudez de, L.M., 2007. A mutant ataxin-3 fragment results from processing at a site N-terminal to amino acid 190 in brain of Machado–Joseph disease-like transgenic mice. Neurobiol Dis 27, 362–369.

Cummings, C.J., Zoghbi, H.Y., 2000. Trinucleotide repeats: mechanisms and pathophysiology. Annu. Rev. Genomics Hum. Genet. 1, 281–328.

Doss-Pepe, E.W., Stenroos, E.S., Johnson, W.G., Madura, K., 2003. Ataxin-3 interactions with rad23 and valosin-containing protein and its associations with ubiquitin chains and the proteasome are consistent with a role in ubiquitin-mediated proteolysis. Mol. Cell. Biol. 23, 6469–6483.

Evers, M.M., Pepers, B.A., van Deutekom, J.C., Mulders, S.A., den Dunnen, J.T., Aartsma-Rus, A., 2011. Targeting several CAG expansion diseases by a single antisense oligonucleotide. PLoS One 6, e24308.

Gaspar, C., Lopes-Cendes, I., Hayes, S., Goto, J., Arvidsson, K., Dias, A., et al., 2001. Ancestral origins of the Machado–Joseph disease mutation: a worldwide haplotype study. Am. J. Hum. Genet. 68, 523–528.

Goemans, N.M., Tulinius, M., van den Akker, J.T., Burm, B.E., Ekhart, P.F., Heuvelmans, N., et al., 2011. Systemic administration of PRO051 in Duchenne's muscular dystrophy. N. Engl. J. Med. 364, 1513–1522.

Goti, D., Katzen, S.M., Mez, J., Kurtis, N., Kiluk, J., Ben-Haiem, L., et al., 2004. A mutant ataxin-3 putative-cleavage fragment in brains of Machado–Joseph disease patients and transgenic mice is cytotoxic above a critical concentration. J. Neurosci. 24, 10266–10279.

Goto, J., Watanabe, M., Ichikawa, Y., Yee, S.B., Ihara, N., Endo, K., et al., 1997. Machado–Joseph disease gene products carrying different carboxyl termini. Neurosci. Res. 28, 373–377.

Haacke, A., Hartl, F.U., Breuer, P., 2007. Calpain inhibition is sufficient to suppress aggregation of polyglutamine-expanded ataxin-3. J. Biol. Chem. 282, 18851–18856.

Hu, J.X., Matsui, M., Gagnon, K.T., Schwartz, J.C., Gabillet, S., Arar, K., et al., 2009. Allele-specific silencing of mutant huntingtin and ataxin-3 genes by targeting expanded CAG repeats in mRNAs. Nat. Biotechnol. 27, 478–484.

Hu, J., Gagnon, K.T., Liu, J., Watts, J.K., Syeda-Nawaz, J., Bennett, C.F., et al., 2011. Allele-selective inhibition of ataxin-3 (ATX3) expression by antisense oligomers and duplex RNAs. Biol. Chem. 392, 315–325.

Hubener, J., Vauti, F., Funke, C., Wolburg, H., Ye, Y., Schmidt, T., et al., 2011. N-terminal ataxin-3 causes neurological symptoms with inclusions, endoplasmic reticulum stress and ribosomal dislocation. Brain 134, 1925–1942.

Ikeda, H., Yamaguchi, M., Sugai, S., Aze, Y., Narumiya, S., Kakizuka, A., 1996. Expanded polyglutamine in the Machado–Joseph disease protein induces cell death *in vitro* and *in vivo*. Nat. Genet. 13, 196–202.

Kordasiewicz, H.B., Stanek, L.M., Wancewicz, E.V., Mazur, C., McAlonis, M.M., Pytel, K.A., et al., 2012. Sustained therapeutic reversal of Huntington's disease by transient repression of huntingtin synthesis. Neuron 74, 1031–1044.

Macedo-Ribeiro, S., Cortes, L., Maciel, P., Carvalho, A.L., 2009. Nucleocytoplasmic shuttling activity of ataxin-3. PLoS One 4, e5834.

Matos, C.A., de Macedo-Ribeiro, S., Carvalho, A.L., 2011. Polyglutamine diseases: the special case of ataxin-3 and Machado–Joseph disease. Prog. Neurobiol. 95, 26–48.

Miller, V.M., Xia, H., Marrs, G.L., Gouvion, C.M., Lee, G., Davidson, B.L., et al., 2003. Allele-specific silencing of dominant disease genes. Proc. Natl. Acad. Sci. U. S. A. 100, 7195–7200.

Nobrega, C., Nascimento-Ferreira, I., Onofre, I., Albuquerque, D., Hirai, H., Deglon, N., et al., 2013. Silencing mutant ataxin-3 rescues motor deficits and neuropathology in Machado–Joseph disease transgenic mice. PLoS One 8, e52396.

Rigo, F., Hua, Y., Krainer, A.R., Bennett, C.F., 2012. Antisense-based therapy for the treatment of spinal muscular atrophy. J. Cell Biol. 199, 21–25.

Rozen, S., Skaletsky, H., 2000. Primer3 on the WWW for general users and for biologist programmers. Methods Mol. Biol. 132, 365–386.

Ruijter, J.M., Ramakers, C., Hoogaars, W.M.H., Karlen, Y., Bakker, O., van den Hoff, M.J.B., 2009. Amplification efficiency: linking baseline and bias in the analysis of quantitative PCR data. Nucleic Acids Res. 37, e45.

Scheel, H., Tomiuk, S., Hofmann, K., 2003. Elucidation of ataxin-3 and ataxin-7 function by integrative bioinformatics. Hum. Mol. Genet. 12, 2845–2852.

Schmitt, I., Linden, M., Khazneh, H., Evert, B.O., Breuer, P., Klockgether, T., et al., 2007. Inactivation of the mouse Atxn3 (ataxin-3) gene increases protein ubiquitination. Biochem. Biophys. Res. Commun. 362, 734–739.

Spitali, P., Aartsma-Rus, A., 2012. Splice modulating therapies for human disease. Cell 148, 1085–1088.

Takahashi, T., Katada, S., Onodera, O., 2010. Polyglutamine diseases: where does toxicity come from? What is toxicity? Where are we going? J. Mol. Cell Biol. 2, 180–191.

Trottier, Y., Lutz, Y., Stevanin, G., Imbert, G., Devys, D., Cancel, G., et al., 1995. Polyglutamine expansion as a pathological epitope in Huntington's disease and 4 dominant cerebellar ataxias. Nature 378, 403–406.

van Putten, M., Aartsma-Rus, A., 2011. Opportunities and challenges for the development of antisense treatment in neuromuscular disorders. Expert. Opin. Biol. Ther. 11, 1025–1037.

Wang, Q., Li, L., Ye, Y., 2006. Regulation of retrotranslocation by p97-associated deubiquitinating enzyme ataxin-3. J. Cell Biol. 174, 963–971.

Warrick, J.M., Morabito, L.M., Bilen, J., Gordesky-Gold, B., Faust, L.Z., Paulson, H.L., et al., 2005. Ataxin-3 suppresses polyglutamine neurodegeneration in *Drosophila* by a ubiquitin-associated mechanism. Mol. Cell 18, 37–48.

Zalachoras, I., Evers, M.M., van Roon-Mom, W.M., Aartsma-Rus, A.M., Meijer, O.C., 2011. Antisense-mediated RNA targeting: versatile and expedient genetic manipulation in the brain. Front. Mol. Neurosci. 4, 10.

Zhang, M.Q., 1998. Statistical features of human exons and their flanking regions. Hum. Mol. Genet. 7, 919–932.